

Did high Neo-Tethys subduction rates contribute to early Cenozoic warming?

G. Hoareau et al.

Did high Neo-Tethys subduction rates contribute to early Cenozoic warming?

G. Hoareau^{1,2}, B. Bomou^{1,3,4}, D. J. J. van Hinsbergen⁵, N. Carry¹, D. Marquer¹, Y. Donnadiou⁴, G. Le Hir³, B. Vrielynck⁶, and A.-V. Walter-Simonnet¹

¹UMR 6249 Chrono-environnement (CNRS-Université de Franche-Comté), 25030 Besançon cedex, France

²UMR CNRS TOTAL 5150 Laboratoire des Fluides Complexes et leurs Réservoirs, Université de Pau et des Pays de l'Adour, I.P.R.A., Avenue de l'Université BP 1155 64013 PAU cedex, France

³Institut de Physique du Globe de Paris, 4 place Jussieu 75005 Paris, France

⁴LSCE/UVSQ/IPSL CEA Saclay, Orme des Merisiers, 91191 Gif-sur-Yvette, France

⁵Department of Earth Sciences, Utrecht University, Budapestlaan 4, 3584 CD Utrecht, the Netherlands

⁶UMR 7193 – ISTEP (CNRS-UPMC), 4 place Jussieu, 75252 Paris cedex 05, France

Received: 28 May 2015 – Accepted: 18 June 2015 – Published: 08 July 2015

Correspondence to: G. Hoareau (guilhem.hoareau@univ-pau.fr)

Published by Copernicus Publications on behalf of the European Geosciences Union.

Title Page

Abstract

Introduction

Conclusions

References

Tables

Figures



Back

Close

Full Screen / Esc

Printer-friendly Version

Interactive Discussion



Abstract

The 58–51 Ma interval was characterized by a long-term increase of global temperatures (+4 to +6 °C) up to the Early Eocene Climate Optimum (EECO, 52.9–50.7 Ma), the warmest interval of the Cenozoic. It was recently suggested that sustained high atmospheric $p\text{CO}_2$, controlling warm early Cenozoic climate, may have been released during Neo-Tethys closure through the subduction of large amounts of pelagic carbonates and their recycling as CO_2 at arc volcanoes (“carbonate subduction factory”). To analyze the impact of Neo-Tethys closure on early Cenozoic warming, we have modeled the volume of subducted sediments and the amount of CO_2 emitted at active arc volcanoes along the northern Tethys margin. The impact of calculated CO_2 fluxes on global temperature during the early Cenozoic have then been tested using a climate carbon cycle model (GEOCLIM). We first show that CO_2 production may have reached up to $1.55 \times 10^{18} \text{ mol Ma}^{-1}$ specifically during the EECO, ~ 4 to 37% higher than the modern global volcanic CO_2 output, owing to a dramatic India–Asia plate convergence increase. In addition to the background CO_2 degassing, the subduction of thick Greater Indian continental margin carbonate sediments at ~ 55 –50 Ma may also have led to additional CO_2 production of $3.35 \times 10^{18} \text{ mol Ma}^{-1}$ during the EECO, making a total of 85% of the global volcanic CO_2 outgassed. However, climate modelling demonstrates that timing of maximum CO_2 release only partially fit with the EECO, and that corresponding maximum $p\text{CO}_2$ values (750 ppm) and surface warming (+2 °C) do not reach values inferred from geochemical proxies, a result consistent with conclusions arise from modelling based on other published CO_2 fluxes. These results demonstrate that CO_2 derived from decarbonation of Neo-Tethyan lithosphere may have possibly contributed to, but certainly cannot account alone for early Cenozoic warming, including the EECO. Other commonly cited sources of excess CO_2 such as enhanced igneous province volcanism also appear to be up to one order of magnitude below fluxes required by the model to fit with proxy data of $p\text{CO}_2$ and temperature at that time.

Did high Neo-Tethys subduction rates contribute to early Cenozoic warming?

G. Hoareau et al.

Title Page

Abstract

Introduction

Conclusions

References

Tables

Figures



Back

Close

Full Screen / Esc

Printer-friendly Version

Interactive Discussion



1 Introduction

Based on paleotemperature proxies, a trend of decreasing global temperatures throughout the Late Mesozoic and Cenozoic has long been identified (e.g. Schackleton and Kennett, 1975; Zachos et al., 2001, 2008; Cramer et al., 2009; Friedrich et al., 2012). Climatic modeling suggests that this cooling mainly results from decreasing seafloor spreading and subduction rates, as well as increasing CO₂ removal through silicate weathering (Park and Royer, 2011; Godd ris et al., 2014; van der Meer et al., 2014). Global cooling was interrupted by a long-term increase of global temperatures (+4 to +6 C) and pCO₂ (~ 450 ppm to ~ 1000 ppm) from 58 to 5.7 Ma, crowned by the Early Eocene Climate Optimum (EECO, 52.9–50.7 Ma), the warmest interval of the Cenozoic (Zachos et al., 2001; Beerling and Royer, 2011). Conventional carbon cycle models fail to reproduce this rise in temperature and atmospheric CO₂ without the addition of excess CO₂ compared to background CO₂ volcanic degassing rates (4–10 × 10¹⁸ molCO₂Ma⁻¹ at present; Berner, 2004) (Lefebvre et al., 2013; Van der Meer et al., 2014). Carbonates also indicate that from ~ 58.0 to 52.5 Ma this warming was characterized by a 3 to 4‰ negative shift in marine and terrestrial δ¹³C, referred to as the Late Paleocene–Early Eocene (LPEE) by Komar et al. (2013). This drop in δ¹³C suggests an additional source of depleted CO₂ (i.e enriched in ¹²C) or/and decreased net organic carbon burial (Hilting et al., 2008; Komar et al., 2013). In contrast, despite warm temperature, the EECO was associated with a rise in δ¹³C (Cramer et al., 2009), indicative of the addition of heavy CO₂ or/and alternatively by increased net organic carbon burial (e.g., Komar et al., 2013). Various origins of excess CO₂ have been proposed for both periods of the early Cenozoic. Most invoke the activity of large igneous provinces such as the North Atlantic Igneous Province (NAIP), since a mantellic source of CO₂ (δ¹³CO₂ ranging from –3 to –10‰) may be compatible with carbon isotope proxies for most of the period of warming (see Reagan et al., 2013 and references therein). Alternatively, Hilting et al. (2008) and Komar et al. (2013) proposed that large amounts of low-δ¹³C organic carbon were being stored in carbon capacitors

Did high Neo-Tethys subduction rates contribute to early Cenozoic warming?

G. Hoareau et al.

Title Page

Abstract

Introduction

Conclusions

References

Tables

Figures



Back

Close

Full Screen / Esc

Printer-friendly Version

Interactive Discussion



separate from the ocean/atmosphere/biosphere (e.g., peat, gas hydrates, permafrost) during the Paleocene. They were then massively released during the LPEE warming and progressively vanished during the EECO (Komar et al., 2013). Finally, among several other hypotheses, it was suggested that Neo-Tethys closure may have strongly controlled Cretaceous and early Cenozoic climates, up to the EECO, through the subduction of tropical pelagic carbonates ($\delta^{13}\text{C} \sim 0\text{‰}$) under the Asian plate and their recycling as CO_2 at arc volcanoes (Edmond and Huh, 2003; Kent and Muttoni, 2008; Johnston et al., 2011). These authors argued that the tropical latitudes of the northern Neo-Tethys could have favoured deposition of carbonate-rich pelagic sediments on the Tethyan seafloor. In detail, Kent and Muttoni (2008) suggested that the Indian plate dominated this “carbonate subduction factory”, with a major decrease in CO_2 production as India and Asia collided some 50 Ma ago. However, the same authors recently concluded for low CO_2 outgassing at the Tethyan arc, mainly as a result of low decarbonation during subduction (Kent and Muttoni, 2013).

In this contribution, we aim to test whether Neo-Tethyan closure, which was obviously associated to widespread arc volcanism, may have had or not an impact on global warming during the LPEE and the EECO, keeping in mind that this hypothesis hardly conforms to available carbon isotope records during the LPEE. To this end, we first use a simple model that calculates the volume of sediments subducted along with Neo-Tethyan oceanic and Greater Indian margin lithospheres, and computes a range of CO_2 fluxes emitted at active arc volcanoes along the northern Neo-Tethys margin. A coupled climate-carbon cycle model (GEOCLIM) is then used to quantify the impact of CO_2 fluxes obtained from our model and that of Kent and Muttoni (2013), on Paleocene/Eocene $p\text{CO}_2$ and atmospheric temperature. Finally, in light of our results, we discuss the relevance of alternate hypotheses commonly cited to explain the LPEE and the EECO.

CPD

11, 2847–2888, 2015

Did high Neo-Tethys subduction rates contribute to early Cenozoic warming?

G. Hoareau et al.

Title Page

Abstract

Introduction

Conclusions

References

Tables

Figures

◀

▶

◀

▶

Back

Close

Full Screen / Esc

Printer-friendly Version

Interactive Discussion



2 Neo-Tethyan history and related arc volcanism

The Neo-Tethys ocean opened westward during the Permian to Triassic, separating several micro-continents (e.g., Pontides, Central Iran, Central Afghanistan, Tibet, and Western Burma) from Gondwana in the south (Kazmin, 1991; Dercourt et al., 1993; Ricou, 1994; Stampfli and Borel, 2002; Muttoni et al., 2009). These reached the southern Eurasian margin in Late Triassic and younger times, followed by inception of subduction of Neo-Tethyan oceanic lithosphere. In the western Neo-Tethys, convergence of Africa to Eurasia began in the Aptian (Kazmin, 1991; Dercourt et al., 1993; Ricou, 1994; Rosenbaum et al., 2002; Stampfli and Borel, 2002; van Hinsbergen et al., 2005) (Fig. 1). Neo-Tethys subduction below the Iran margin started at least in Jurassic time and continued until Arabia–Eurasia collision in latest Eocene–Early Oligocene time (Agard et al., 2011; Mouthereau, 2011; McQuarrie and van Hinsbergen, 2013). Subduction below Tibet in the Early Cretaceous occurred simultaneously with Indian separation from eastern Antarctica and Australia ~ 130 Ma ago (Guillot et al., 2008; van Hinsbergen et al., 2011a). Collision between the northernmost continental crust of the Indian plate and Eurasia is commonly stated to have started at ~ 55–50 Ma (e.g., Dupont-Nivet et al., 2010; Najman et al., 2010; Orme et al., 2015) (Fig. 1). At about the same time (~ 56–47 Ma), subducted Indian northern margin rocks were affected by High-Pressure and Ultra-High Pressure metamorphism (up to ~ 100 km depth) (Guillot et al., 2008). In the easternmost Neo-Tethys (Indonesia), Whittaker et al. (2007) suggested that active subduction below Eurasia was active throughout the Upper Cretaceous and the Cenozoic, although Hall (2012) proposed that Sundaland was mostly surrounded by inactive, or transform margins from 90 to 45 Ma. Finally, there is also documentation for multiple intra-oceanic subduction events leading to widespread ophiolite obduction, ending around 70 Ma along NE Arabia, and around 55–50 Ma in SE Oman, Pakistan (Gnos et al., 1997; Marquer et al., 1998; Gaina et al., 2015), and the Tibetan Himalaya (Hébert et al., 2012; Garzanti and Hu, 2015; Huang et al., 2015a) (Fig. 1).

Did high Neo-Tethys subduction rates contribute to early Cenozoic warming?

G. Hoareau et al.

Title Page

Abstract

Introduction

Conclusions

References

Tables

Figures



Back

Close

Full Screen / Esc

Printer-friendly Version

Interactive Discussion



Did high Neo-Tethys subduction rates contribute to early Cenozoic warming?

G. Hoareau et al.

Title Page

Abstract

Introduction

Conclusions

References

Tables

Figures



Back

Close

Full Screen / Esc

Printer-friendly Version

Interactive Discussion



Evidence of latest Cretaceous and early Cenozoic subduction-related magmatic activity is widespread along, and restricted to the Eurasian margin. For example, in the Zagros mountains and Turkey (Pontides), widespread arc magmatism occurred during the Mesozoic and the Cenozoic (Sengör et al., 1988; Okay and Şahintürk, 1997; Barrier and Vrielynck, 2008; Agard et al., 2011; Eyuboglu et al., 2011). In southern Tibet, a long-lasting volcanic “Gangdese” arc was active from Early Cretaceous to Eocene time (Ji et al., 2009), with a short-lived ignimbrite flare-up stage around 50 Ma coinciding with Tibetan Himalaya-Lhasa continental collision (Ji et al., 2009), followed by return of the arc to a background state until the Late Eocene (Sanchez et al., 2013). In Sundaland, Paleocene-Eocene magmatism was likely active since at least ~ 63 Ma (e.g., McCourt et al., 1996; Bellon et al., 2004).

3 Volcanic CO₂ release during the LPEE and the EECO by the Carbonate Subduction Factory Model (CSFM)

CSFM is designed to calculate the amount of CO₂ produced during Neo-Tethys closure. It quantifies the Neo-Tethys volcanic arc gas output as a function of subduction flux of oceanic crust, pelagic sediments, and also of Indian margin sediments at the onset of Indian continental lithosphere subduction. Required input parameters are subduction rate, trench length, the thickness, density, carbonate and organic carbon content of sediments and oceanic crust, the decarbonation efficiency of subducted material, and the time-lag to gas emission at the surface.

3.1 Subduction rates and trench length estimates

Subduction rates of African, Arabian and Indian plates below Eurasia were calculated from plate motion reconstructions made with GPlates (<http://www.gplates.org/>) (Boyd et al., 2011) using time steps of 0.5 Ma, between 65 and 35 Ma. Given the controversy regarding the presence or not of continuous subduction in easternmost Neo-

Did high Neo-Tethys subduction rates contribute to early Cenozoic warming?

G. Hoareau et al.

Title Page

Abstract

Introduction

Conclusions

References

Tables

Figures



Back

Close

Full Screen / Esc

Printer-friendly Version

Interactive Discussion



Tethys from the Late Cenozoic to the Eocene (Sundaland) (e.g., Whittaker et al., 2007; Hall, 2012), we did not consider Australia–Eurasia convergence and assess the potential role of Neotethys subduction based on the central and western Neotethys alone. We used the reconstructed position of three points located on the western, central and eastern syntaxis of each plate, similar to Rosenbaum et al. (2002), Alvarez (2010) and van Hinsbergen et al. (2011a). Their present locations in Lat/Long decimal coordinates are 37/15, 32/24, 24/32 (Africa), 24.1/32.9, 15.3/38.9, 23.6/58.6 (Arabia) and 30.5/72, 30.5/82, 23.5/92 (India). Euler rotation parameters were taken from plate circuit A of van Hinsbergen et al. (2011a). Because Cretaceous–Cenozoic intra-Eurasian shortening north of the African–Arabian plate is limited to perhaps 200 km and focused in the late Cenozoic (e.g., Mouthereau, 2011; McQuarrie and van Hinsbergen, 2013), we considered Africa/Arabia–Eurasia convergence rates as subduction rates. For India, the subduction rate was calculated subtracting intra-Asian shortening rates expressed as Euler rotation parameters by van Hinsbergen et al. (2011b) from India–Asia convergence rates. Given the uncertainties concerning the rate of subduction below widespread ophiolites, and the locations of these subduction zones, we chose to simplify our scenario by assigning all subduction to the zones indicated in Fig. 1. In addition, we assume that there was no active spreading within the Neo-Tethys since 65 Ma. For each plate, subduction rates at each time step were corrected for convergence obliquity related to the orientation of the subduction trench (Appendix A). Trench lengths were set to 2500 km for Africa, 2900 km for Arabia (from the Levant fault to the Makran) and 2600 km for India (from the Makran to the Indo-Burma range), making a total length of 8000 km (similar to Johnston et al., 2011) (Fig. 1). Three ages, 55, 52.5 and 50 Ma, were tested for the onset of Greater Indian thinned continental lithosphere subduction beneath Eurasia, corresponding to a shift from pelagic to margin sediments on the Indian plate. Scenarios without India–Asia continental subduction were also run, to assess the maximum potential effects of younger collision.

tions of syn-rift/post-rift Neo-Tethyan margin sediment thicknesses of Sciunnach and Garzanti (2012). Although the lithology of the margin was variable, the proportion of carbonate sediments and organic matter may have been important (Beck et al., 1995; Liu and Einsele, 1994; Sciunnach and Garzanti, 2012). Average contents of 50 and 1 wt% were chosen for carbonate and organic carbon content, respectively. Uncompacted margin sediments were given a density of 2 tm^{-3} as calculated from data of Sciunnach and Garzanti (2012).

3.3 Decarbonation efficiency of subducted materials

3.3.1 Oceanic crust and pelagic sediments

In the “carbonate subduction factory” model, CO_2 produced during oceanic subduction processes originates from deep metamorphic decarbonation of subducted crust and sediments (carbonate and organic matter), and is assumed to be released at volcanic arcs following partial melting of the subducting oceanic crust and metasomatism of the overlying mantle (Hilton et al., 2002; Gorman et al., 2006). This common statement was followed in the CSFM model (Fig. 3), therefore ignoring possible additional CO_2 sources, in particular decarbonation of the overlying crust (Lee et al., 2013). The amount of CO_2 released through arc volcanism was calculated as follows: first, for each time step, the total volume of subducting sediment and crust was computed. We assumed this volume to be similar to that encompassing metamorphic carbon loss in the sub-arc zone ($\sim 120 \pm 40 \text{ km}$ depth; England and Katz, 2010) (i.e., no variation of volume during the subduction process before decarbonation). Then, the amount of CO_2 emitted at the surface was estimated following the approach of Johnston et al. (2011), who recently re-calculated modern decarbonation efficiencies at sub-arc depth (Appendix B). Their estimations vary from 0.1 to 70% efficiency, with most values ranging between 18 and 54%. We have retained values of 15 to 60%. The time lag between decarbonation at depth and gas emission at the surface was set to 2 Ma, averaging time scales of Turner (2002) (0.4 to 4 Ma).

Did high Neo-Tethys subduction rates contribute to early Cenozoic warming?

G. Hoareau et al.

Title Page	
Abstract	Introduction
Conclusions	References
Tables	Figures
⏪	⏩
◀	▶
Back	Close
Full Screen / Esc	
Printer-friendly Version	
Interactive Discussion	



3.3.2 Continental crust and Indian margin sediments

Due to the lack of aqueous fluids in continental crust, continental subduction zones are expected to be devoid of significant syn-subduction arc volcanism in the overlying plate (Zheng, 2012). Although volcanism may have continued in Tibet after 50 Ma (Ji et al., 2009; Rohrman et al., 2012), in the model oceanic slab-related metamorphic decarbonation and magma generation was considered to last until the arrival of the continental lithosphere at sub-arc depth (i.e., 80 km) (Fig. 3) Using preferred geometric parameters of Leech et al. (2005) for subduction of the Indian plate, this depth is reached ~ 1.5 to 2 Ma after the initiation of continental subduction. Despite cessation of volcanic activity, subduction of continental margin sediments may have been associated to active CO_2 degassing at springs or vents as a result of efficient metamorphic sediment decarbonation at $T > 300^\circ\text{C}$ (e.g., Becker et al., 2008; Evans et al., 2008). Kerrick and Caldeira (1993) suggested that limited collision-related prograde metamorphism of marly lithologies may induce a CO_2 loss of ~ 10 wt %, equivalent to a decarbonation efficiency of ~ 50 % for sediments with a carbonate content of 50 wt % (= 22 wt % CO_2). This value may represent an upper estimate as shown by thermodynamic modeling of Massonne (2010). Above-mentioned studies focus on collision rather than continental subduction, for which to our knowledge no estimations of CO_2 outgassing fluxes or decarbonation efficiency are available. To avoid overestimations of CO_2 production, we assumed that only limited margin sediment decarbonation may have occurred after the onset of continental subduction at low-grade conditions, with a 1 to 10 wt % efficiency. Time necessary for subducted margin material to reach the 300°C isotherm after the onset of continental subduction at 55–50 Ma (corresponding to 25 km depth with a normal-subduction geothermal gradient of 15°C km^{-1}) was set to 0.5 Ma, as calculated with parameters of Leech et al. (2005). Circulation of CO_2 -rich fluids along large-scale collision-related thrust detachments has been proposed as an efficient way to promote degassing at the surface (e.g., Kerrick and Caldeira, 1993; Becker et al., 2008). Following Skelton (2011), who suggested that gas produced dur-

Did high Neo-Tethys subduction rates contribute to early Cenozoic warming?

G. Hoareau et al.

Title Page

Abstract

Introduction

Conclusions

References

Tables

Figures

◀

▶

◀

▶

Back

Close

Full Screen / Esc

Printer-friendly Version

Interactive Discussion



ing low-grade metamorphism may be rapidly released to the surface (~ 4000 yr), we considered immediate release of CO_2 to the atmosphere (Appendix B).

3.4 Results

3.4.1 Tethyan subduction rate

5 During the Paleocene (65 to 56 Ma), the mean subduction rate (i.e., all plates) has a constant value of $\approx 5.5 \text{ cm yr}^{-1}$ (Fig. 4a). Increased rates (up to 8.3 cm yr^{-1}) are computed between 56 and 53 Ma, before a gradual decrease to 3 cm yr^{-1} at 35 Ma. Similar results are obtained with rotation parameters of Müller et al. (2008). India–Asia convergence, which reaches up to 16.7 cm yr^{-1} at 53–52 Ma, exerts the main control on high
10 early Cenozoic subduction rates.

3.4.2 Greenhouse gas production

It is important to note that decarbonation efficiencies may have strongly varied with time, depending particularly on the plate age and sediment thickness (Peacock, 2003; Gorman et al., 2006; Johnston et al., 2011). However, according to Johnston
15 et al. (2011) the decarbonation efficiency is only roughly correlated with convergence (subduction) rate. Therefore, excess CO_2 fluxes calculated at minimum (15%) and maximum (60%) efficiencies correspond to extreme scenarios that very likely encompass true excess CO_2 fluxes related to Neo-Tethys closure.

Without Indian continental subduction

20 If Greater Indian continental subduction collision is not considered, CO_2 production varies from $0.3\text{--}1.1 \times 10^{18}$ to $0.4\text{--}1.65 \times 10^{18} \text{ mol CO}_2 \text{ Ma}^{-1}$ (15–60% efficiency, respectively) between 65 and 50 Ma (Fig. 4b). This amounts up to 37% of the modern global outgassing rate ($\sim 4\text{--}10 \times 10^{18} \text{ mol CO}_2 \text{ Ma}^{-1}$; Berner, 2004). Highest possible values occur at a peak centered on the EECO (54–51 Ma). These flow rates exceed

Did high Neo-Tethys subduction rates contribute to early Cenozoic warming?

G. Hoareau et al.

Title Page

Abstract

Introduction

Conclusions

References

Tables

Figures

◀

▶

◀

▶

Back

Close

Full Screen / Esc

Printer-friendly Version

Interactive Discussion



those computed before 65 Ma and after 50 Ma. If subduction of the Indian plate alone was acting as the main driver of CO₂ degassing, as proposed by Kent and Muttoni (2008), maximal CO₂ production would reach 1.1 × 10¹⁸ mol CO₂ Ma⁻¹ from 54 to 50 Ma (Fig. 4c), corresponding to 11–27 % of the modern outgassing rate.

5 With Indian continental subduction

Decarbonation of Greater Indian margin sediments, added to the last volumes of pelagic sediments at sub-arc depth, results in a peak of CO₂ production ~ 2 Ma after the onset of continental subduction, considering a constant decarbonation efficiency (Fig. 4d). In our model, continental subduction must start at 52.5 Ma (consistent for example with stratigraphic arguments of Najman et al., 2010 and paleomagnetic arguments of Huang et al., 2015b) for maximum CO₂ emissions to occur at ~ 51 Ma, i.e. coeval to maximum recorded temperatures during the EECO (Zachos et al., 2008). In this case, CO₂ degassing flow rates are in the range 0.6–3.35 × 10¹⁸ mol CO₂ Ma⁻¹ (1/15–10/60 % efficiencies for margin/pelagic sediments, respectively), corresponding to 6–84 % of the modern CO₂ outgassing rate. A 55 Ma age for the inset of continental subduction results in even higher production (0.65–3.7 × 10¹⁸ mol CO₂ Ma⁻¹) although on a peak centered at 53.5 Ma, ~ 2 Ma before maximum recorded paleotemperatures (Fig. 4d). In contrast, late subduction (50 Ma) results in the presence of two smaller peaks: the first one (54–52 Ma) only relates to decarbonation of subducted pelagic sediments whereas the second (48–46 Ma) largely results from decarbonation of margin sediments (0.32–2 × 10¹⁸ mol CO₂ Ma⁻¹ for 1–10 % efficiency, respectively) (Fig. 4d). If the Indian plate alone is considered (52.5 Ma), CO₂ production reaches 0.46–3 × 10¹⁸ mol CO₂ Ma⁻¹ (1/15–10/60 % efficiencies for margin/pelagic sediments, respectively) at ~ 52–51 Ma, amounting up to 75 % of the modern outgassing rate (Fig. 4e).

CPD

11, 2847–2888, 2015

Did high Neo-Tethys subduction rates contribute to early Cenozoic warming?

G. Hoareau et al.

Title Page

Abstract

Introduction

Conclusions

References

Tables

Figures



Back

Close

Full Screen / Esc

Printer-friendly Version

Interactive Discussion



4 Modeling the impact of Neo-Thetys closure

To test the influence of calculated excess CO₂ fluxes on Paleocene/Early Eocene climate, we carried out simulations using the GEOCLIM model (Donnadieu et al., 2004; Godd ris et al., 2008). This model couples a 3-D General Circulation model (GCM) called FOAM (Jacob, 1997) to a box model of geological carbon-alkalinity cycles called COMBINE (Godd ris and Joachimski, 2004). The GCM FOAM is used in mixed-layer mode, where atmosphere is linked to a 50 m mixed-layer ocean, which parameterizes heat transport through diffusion, in order to reduce computation time (one GEOCLIM simulation needs up to 12 GCM simulations). This GCM is forced by a large range of pCO₂ (200 up to 4200 ppmv) to generate an offline catalogue of continental air temperature and continental runoff with a spatial resolution of 7.5° long × 4.5° lat. For each corresponding atmospheric pCO₂ value, the GEOCLIM model calculates the temperature and the runoff of each grid cell through a linear interpolation procedure from the climatic catalogue. This procedure is repeated until a steady-state is reached that corresponds to a stable atmospheric CO₂ and temperature. The model uses an ocean geometry divided into two polar oceans (including a photic zone and a deep ocean reservoir), a low- to mid-latitude ocean (including a photic zone, a thermocline and a deep ocean reservoir), two epicontinental seas (both with a photic zone and a deep epicontinental reservoir) and the atmosphere. A full description of GEOCLIM and its components COMBINE and FOAM can be found in Godd ris and Joachimski (2004) and Donnadieu et al. (2006).

4.1 GEOCLIM simulations

We first calculated the steady-state pCO₂, assuming that the total CO₂ consumed by continental silicate rocks weathering equals the total solid Earth CO₂ degassing flux (Walker et al., 1981). Due to the non-consensus about the Earth degassing rate for the last 200 Ma, the degassing flux was assumed constant and fixed at a modern value of $6.8 \times 10^{18} \text{ mol CO}_2 \text{ Ma}^{-1}$, which is required in the model to balance the global con-

Did high Neo-Tethys subduction rates contribute to early Cenozoic warming?

G. Hoareau et al.

Title Page

Abstract

Introduction

Conclusions

References

Tables

Figures



Back

Close

Full Screen / Esc

Printer-friendly Version

Interactive Discussion



Did high Neo-Tethys subduction rates contribute to early Cenozoic warming?

G. Hoareau et al.

[Title Page](#)[Abstract](#)[Introduction](#)[Conclusions](#)[References](#)[Tables](#)[Figures](#)[Back](#)[Close](#)[Full Screen / Esc](#)[Printer-friendly Version](#)[Interactive Discussion](#)

sumption through the weathering of silicate lithologies (Donnadiou et al., 2006). Each terrestrial grid was prescribed a similar lithology, in which basalt weathering reaches a 30 % contribution of the total silicate weathering flux taken at present day (Dessert et al., 2003) (similar to UNI configuration of Lefebvre et al., 2013). Lefebvre et al. (2013) have shown that with this configuration steady-state $p\text{CO}_2$ is similar at 65, 52 and 30 Ma (320–350 ppm), despite variations in paleogeography. An Early Eocene (52 Ma) paleogeographic reconstruction was thus used in the simulation, which runs from 65 to 40 Ma. Land-ocean configuration was built from a synthesis of paleomagnetic data and geologic constraints (Besse and Courtillot, 2002; Dercourt et al., 1993). Obliquity and radiation solar constant were assumed to equal present-day values.

The main geological forcing tested in the simulation is the additional CO_2 fluxes calculated from CFSM. CO_2 fluxes of Kent and Muttoni (2013) have also been tested, using decarbonation efficiencies of 15 and 60 % in addition to the original value of 10 % proposed by the authors. Computed CO_2 outgassing rates resulting from Neo-Tethys closure were integrated to GEOCLIM, in an age step of 1 Ma.

4.2 $p\text{CO}_2$ evolution during the LPEE and the EECO

If minimum decarbonation efficiency (15 %) is considered, $p\text{CO}_2$ increase following excess CO_2 flux is negligible (Fig. 5c). For example, the addition of continental subduction, which results in higher CO_2 fluxes, allows reaching maximum $p\text{CO}_2$ of only 360–365 ppm at 51 Ma (i.e. close to steady state values).

If maximum decarbonation efficiency (60 %) is considered, calculated excess CO_2 fluxes lead to $p\text{CO}_2$ of 430–450 ppm from 65 to 54 Ma (Fig. 5c). Without continental subduction, between 54 and 51 Ma, $p\text{CO}_2$ increases up to 500–550 ppm. It then decreases to steady state $p\text{CO}_2$ values from 48 Ma. With continental subduction, $p\text{CO}_2$ can reach much higher values. In the preferred scenario (initiation of continental subduction at 52.5 Ma), $p\text{CO}_2$ strongly increases at 54 Ma up to reach a peak of ~ 770 ppm at 51.5 Ma. It then decreases to values close to steady state at 47 Ma (Fig. 5c). If continental subduction begins at 55 Ma, a peak of similar amplitude (770 ppm) occurs at

53 Ma (Fig. 5d). In contrast, a 50 Ma age for the initiation of subduction results in two peaks of smaller amplitude, with $p\text{CO}_2$ values of ~ 520 and ~ 570 ppm at ~ 52 and 48 Ma, respectively (Fig. 5d).

Using excess CO_2 fluxes of Kent and Muttoni (2013) leads to low atmospheric CO_2 concentrations whatever chosen decarbonation efficiencies (10, 15 or 60 %) (Fig. 5e). Following an increasing trend of excess CO_2 flux, $p\text{CO}_2$ progressively increases from 330-340-445 ppm at 65 Ma to 335-345-475 ppm at 50 Ma (10-15-60 % efficiency, respectively). It then decreases rapidly to values lower than 335 ppm after 48 Ma.

5 Discussion

5.1 Impact of Neo-Tethys closure on Paleocene/Eocene climate

It has long been suggested that Paleocene/Eocene warming was not due to an increase of mantle degassing, calling for additional sources of atmospheric CO_2 (Engelbreton et al., 1992; Kerrick and Caldeira, 1993; Hilting et al., 2008; Van der Meer et al., 2014). Kerrick and Caldeira (1993) first showed, on the basis of a simple carbon cycle model that the minimal value of additional CO_2 necessary to drive climate warming during the LPEE and the EECO ($\geq 1^\circ\text{C}$) may have been close to $\sim 10^{18} \text{ mol CO}_2 \text{ Ma}^{-1}$. More recently, Lefebvre et al. (2013) used the GEOCLIM model to calculate that a higher flux of $\sim 3.4 \times 10^{18} \text{ mol CO}_2 \text{ Ma}^{-1}$, corresponding to a 50 % increase of global CO_2 degassing rate, was needed to reach a $p\text{CO}_2$ value of 930 ppm consistent with geochemical proxies compiled by Beerling and Royer (2011).

Estimations of CO_2 outgassing resulting from Neo-Tethys closure during the Cretaceous and the Paleogene have been previously proposed by Edmond and Huh (2003), Johnston et al. (2011) and Kent and Muttoni (2013). Values calculated from data of Kent and Muttoni (2013) ($< 1.3 \times 10^{17} \text{ mol CO}_2 \text{ Ma}^{-1}$ from 80 to 50 Ma) fall largely below those required by modeling of Lefebvre et al. (2013) to reach estimated $p\text{CO}_2$, largely

Did high Neo-Tethys subduction rates contribute to early Cenozoic warming?

G. Hoareau et al.

Title Page

Abstract

Introduction

Conclusions

References

Tables

Figures



Back

Close

Full Screen / Esc

Printer-friendly Version

Interactive Discussion



because of their choice of limited decarbonation efficiency during subduction (10%). In contrast, estimations of Edmond and Huh (2003) and Johnston et al. (2011) vary from 0.5 to 4×10^{18} molCO₂ Ma⁻¹ for the entire Tethyan arc. According to results of Lefebvre et al. (2013), the higher range of these values should allow to sustain a warm climate during the Paleocene and the lower Eocene. However, excess CO₂ flux calculations of Edmond and Huh (2003) and Johnston et al. (2011) represent only average values based on simple assumptions such as a constant subduction rate for the entire Upper Cretaceous–Lower Cenozoic. Nevertheless, these estimates are generally higher than those calculated using CFSM. We rather suggest that between 65 and ~ 55 Ma (i.e., before the oldest possible age of Indian continental subduction), Neo-Tethys closure may have released less than $\sim 10^{18}$ molCO₂ Ma⁻¹, in particular owing to subduction rates lower than the one used by Edmond and Huh (2003) and Johnston et al. (2011) (~ 5.5 vs. 8 cm yr⁻¹, respectively). Using the GEOCLIM model, CO₂ outgassing values obtained with maximum decarbonation efficiency (60%) allow to reach a *p*CO₂ of ~ 430 ppm, which is in agreement with proxies for the Early Paleocene (65–60 Ma) (Beerling and Royer, 2011) (Fig. 5c). Therefore, our modeling suggests that high decarbonation efficiency was a prerequisite for the “carbonate subduction factory” to have a significant impact on global climate at that time. In addition, GEOCLIM seems unable to explain the onset of Paleocene/Eocene warming at 58 Ma, coevally to an increase of atmospheric *p*CO₂ (Beerling and Royer, 2011) (Fig. 5a–c). Similar conclusions can be drawn from climatic simulations performed with excess CO₂ fluxes of Kent and Muttoni (2013), even using a decarbonation efficiency of 60% (Fig. 5e). In that case, *p*CO₂ only steadily increases during the Paleocene and remains lower than values suggested by proxies (Fig. 5c).

A more significant contribution of Neo-Tethyan closure to global warming may have occurred close to the EECO (~ 52–49 Ma), owing in particular to an increase of the Indian subduction rate (Fig. 4a). This contribution is also conditioned by maximum decarbonation efficiency, and by the onset of Indian continental subduction at ~ 52 Ma. With these two conditions fulfilled, the model allows to reach *p*CO₂ values lower than,

CPD

11, 2847–2888, 2015

Did high Neo-Tethys subduction rates contribute to early Cenozoic warming?

G. Hoareau et al.

Title Page

Abstract

Introduction

Conclusions

References

Tables

Figures



Back

Close

Full Screen / Esc

Printer-friendly Version

Interactive Discussion



Did high Neo-Tethys subduction rates contribute to early Cenozoic warming?

G. Hoareau et al.

Title Page

Abstract

Introduction

Conclusions

References

Tables

Figures



Back

Close

Full Screen / Esc

Printer-friendly Version

Interactive Discussion



but close to proxy ones (< 850 ppm vs. ~ 1000 ppm, respectively) (Fig. 5b). Based on calculations of climate sensitivity to atmospheric CO_2 of GEOCLIM performed by Godderis et al. (2014) (2.4°C for a $p\text{CO}_2$ doubling at 52 Ma), they may have resulted in a related global atmospheric temperature increase of $\sim 2^\circ\text{C}$ compared to the Paleocene.

5 In contrast, if India–Asia continental subduction occurred much later (i.e., equivalent to no collision), Neo-Tethys contribution to the EECO remained negligible, even with a decarbonation efficiency of 60 % (Fig. 5c). Calculations performed with input data of Kent and Muttoni (2013) lead to the same interpretation for the Early Eocene (Fig. 5e).

10 Finally, our study allows to clearly moderate the impact of the Neo-Tethyan “carbonate subduction factory” on Paleocene/Eocene greenhouse, at odds with Edmond and Huh (2003), Johnston et al. (2011) and Kent and Muttoni (2008), but in accordance with recent conclusions of Kent and Muttoni (2013) and Lee et al. (2013).

5.2 Potential additional sources of atmospheric carbon dioxide

5.2.1 Large igneous provinces

15 Since the role of Neo-Tethys closure on the onset of the LPEE and the EECO likely has been limited, other sources of excess greenhouse gases should be called for. These should ideally explain the decrease of marine and terrestrial $\delta^{13}\text{C}$ during the LPEE, and its slight increase during the EECO (Zachos et al., 2001) (Fig. 5a). Numerous geological explanations have been previously postulated for the entire early
20 Cenozoic greenhouse, among which a flare up in the activity of igneous provinces is the most common (e.g., Eldhom and Thomas, 1993; Reagan et al., 2013). Reagan et al. (2013) presented a review of Late Paleocene to Early Eocene magmatism, characterized by the significant activity of at least three major igneous provinces: the North Atlantic Igneous Province, the Siletzia terrane of the northwestern United States and
25 the Yakutat block in southern Alaska. Added to enhanced activity of Neo-Tethys and eastern Pacific subduction-related volcanism, Reagan et al. (2013) concluded for an overall excess CO_2 production of $\sim 2.3 \times 10^{18}$ mol CO_2 for the late Paleocene–Early

Eocene period. Even though this value may appear important, it encompasses time duration of several million years. Assuming a 10 Ma duration for significant magmatism (see Reagan et al., 2013, Fig. 6), the calculated excess CO_2 flow rate falls to only $\sim 2.3 \times 10^{17} \text{ mol CO}_2 \text{ Ma}^{-1}$ on average, one order of magnitude below fluxes necessary to reach a $p\text{CO}_2$ comparable to proxies using the GEOCLIM model. This value can be compared to that of Eldholm and Thomas (1993), who calculated that more than $2.3 \times 10^{18} \text{ mol CO}_2$ may have been released to the atmosphere by the NAIP only, from 58 to 52 Ma (revised to 61–53 Ma by Menzies et al., 2002), corresponding to a flux of $\sim 3 \times 10^{17} \text{ mol CO}_2 \text{ Ma}^{-1}$. We infer, on the base of GEOCLIM modeling, that the effect of enhanced magmatic activity on LPEE warming and the EECO may also have been limited, unless related fluxes have been severely underestimated in the literature. As discussed later, this conclusion is consistent with previous studies of carbon cycle dynamics during the early Cenozoic (e.g., Hilting et al., 2008; Komar et al., 2013).

5.2.2 Metamorphic decarbonation

Lee et al. (2013) argued that the decarbonation of platform carbonates stored on the continental upper plate during subduction-related magmatism may have been far more efficient in driving early Cenozoic greenhouse than the activity of igneous provinces or of the “subduction factory”. Lee et al. (2013) calculated that global CO_2 degassing could have reached 3.7–5.5 times the present day value from during from ~ 140 to 50 Ma, making $2.2\text{--}3.7 \times 10^{19} \text{ mol CO}_2 \text{ Ma}^{-1}$ for a present day value of $6.8 \times 10^{18} \text{ mol CO}_2 \text{ Ma}^{-1}$ (as calculated with GEOCLIM). Cooling initiation during the late Eocene would then have resulted from a transition from a continental-dominated to an island arc-dominated world ca. 52 Ma. The EECO would represent a “last spurt of CO_2 production associated with an Eocene magmatic flare-up in western North America”, based on previous work of Nesbitt et al. (1995) and Kerrick and Caldeira (1998). In light of the GEOCLIM model, we argue that CO_2 fluxes of Lee et al. (2013) are clearly overestimated for the EECO, as $p\text{CO}_2$ close to proxies would be obtained

Did high Neo-Tethys subduction rates contribute to early Cenozoic warming?

G. Hoareau et al.

[Title Page](#)

[Abstract](#)

[Introduction](#)

[Conclusions](#)

[References](#)

[Tables](#)

[Figures](#)



[Back](#)

[Close](#)

[Full Screen / Esc](#)

[Printer-friendly Version](#)

[Interactive Discussion](#)



for excess fluxes lower by approximately one order of magnitude. If they are applied to the EECO, fluxes calculated by Kerrick and Caldeira (1998) for the 60–55 Ma period ($3 \times 10^{18} \text{ mol CO}_2 \text{ Ma}^{-1}$) seem more reasonable. Similar to the decarbonation of pelagic carbonate sediments, crustal decarbonation related to magmatic or metamorphic events should lead to a positive shift of exogenic $\delta^{13}\text{C}$ (Lee et al., 2013), in agreement with proxies for the EECO. In contrast, the LPEE was characterized by a related negative shift in $\delta^{13}\text{C}$ (Zachos et al., 2001), suggesting additional or alternate sources of excess isotopically-light CO_2 .

5.2.3 Organic carbon sources

Several authors have thus proposed organic carbon to be a significant source of excess CO_2 during the LPEE and/or the EECO, mostly based on carbon cycle models (e.g., Kurtz et al., 2003; Hilting et al., 2008; Kroeger and Funnel, 2012; Komar et al., 2013). For example, Kroeger and Funnel (2012) suggested that important reservoir petroleum generation was concurrent with Eocene warming, causing a climate feedback effect through the release of ^{13}C -depleted CO_2 and CH_4 . However, the timing of maximum hydrocarbon production likely occurred during the EECO, which is hardly reconcilable with coeval increase in marine $\delta^{13}\text{C}$ unless net organic carbon burial was significantly higher than during the LPEE (e.g., Kurtz et al., 2003).

The importance of organic carbon dynamics was clearly highlighted by Hilting et al. (2008) who used a carbon cycle model tuned with marine $\delta^{13}\text{C}$ data to calculate Paleocene and Eocene $p\text{CO}_2$ values. These authors managed to reproduce $p\text{CO}_2$ values globally consistent with observations, even though background volcanic/metamorphic CO_2 degassing was kept constant. According to their simulation, large changes in $p\text{CO}_2$ (and thus, temperature) may occur independently of the endogenic carbon cycle. Similar conclusions were drawn by Komar et al. (2013) on the basis of coupled LOSCAR-GEOCARB carbon cycle modeling. They showed that a mantellic source of excess CO_2 during the LPEE would have led to a deepening of the CCD much more important than evidenced from observations. Although based on a different

Did high Neo-Tethys subduction rates contribute to early Cenozoic warming?

G. Hoareau et al.

Title Page

Abstract

Introduction

Conclusions

References

Tables

Figures

◀

▶

◀

▶

Back

Close

Full Screen / Esc

Printer-friendly Version

Interactive Discussion



Did high Neo-Tethys subduction rates contribute to early Cenozoic warming?

G. Hoareau et al.

Title Page

Abstract

Introduction

Conclusions

References

Tables

Figures



Back

Close

Full Screen / Esc

Printer-friendly Version

Interactive Discussion



approach, this conclusion is in good accordance with our suggestion of a moderate impact of LIPs on the LPEE (and the EECO). Instead, Komar et al. (2013) proposed that perturbations of the carbon cycle observed during the LPEE were likely controlled by decrease of net organic carbon burial (either through increased oxidation of organic carbon such as methane hydrates, or through decreased organic carbon burial). In contrast, the rise in marine $\delta^{13}\text{C}$ from 52.5 to 50 Ma suggests that the EECO was characterized by increased net organic carbon burial (as proposed by Komar et al., 2013, with the methane hydrate hypothesis), or as we test in this paper, by the addition of excess CO_2 derived from one or several sources with heavier $\delta^{13}\text{C}$ signatures. Both explanations need to be tested in more detail and reconciled with recent observations that silicate weathering may have been reduced during the EECO, as discussed below.

5.3 Are modeled silicate weathering fluxes overestimated for the EECO?

Most carbon cycle models agree that during the Early Eocene volcanic degassing alone was insufficient to sustain the high $p\text{CO}_2$ values required by proxies, due to important weathering rates at that time (e.g., Berner, 2006; Lefebvre et al., 2013; Komar et al., 2013). For example, Berner (2006) found, based on the time evolution of seawater $^{87}\text{Sr}/^{86}\text{Sr}$ that weathering was mainly controlled by increased basaltic alteration, resulting in a $p\text{CO}_2$ of ~ 700 ppm at 50 Ma, i.e. lower than observations (~ 1000 ppm). Indeed, decreasing of seawater Sr isotopic signature during the Paleocene and the Early Eocene is consistent with the alteration of igneous provinces such as the Deccan Traps or the NAIP (Hodel et al., 2007). In detail, most paleogeographic reconstructions show that the highly weatherable Deccan traps reached the equatorial humid belt (between 5°S and 5°N), where weathering is maximum, at ~ 55 Ma, with a maximum of area between ~ 50 and ~ 35 Ma (Dercourt et al., 1993; Besse and Courtillot, 2002; Van Hinsbergen et al., 2011a, 2012). Accordingly, taking explicitly into account the impact of paleogeography on the long term carbon cycle as done by the GEOCLIM model has led Lefebvre et al. (2013) to suggest that the EECO was characterized by high weathering rates related to weathering of the Deccan traps. As a consequence, the

Did high Neo-Tethys subduction rates contribute to early Cenozoic warming?

G. Hoareau et al.

Title Page

Abstract

Introduction

Conclusions

References

Tables

Figures



Back

Close

Full Screen / Esc

Printer-friendly Version

Interactive Discussion



the end of the EECO. Note that for the LPEE, this interpretation is in contradiction with that of Komar et al. (2013) based on the CCD. In addition, recent modeling of Vigier and Godd ris (2015) suggests that the oceanic $\delta^7\text{Li}$ record of the Early Eocene could equally be explained by intense soil production rates (i.e, intense chemical weathering).

5 These contradictory observations show that the intensity of silicate weathering during the EECO still suffers from strong uncertainties. Additional proxy-based observations are thus needed to calibrate weathering rate values obtained from models, which still lack the explicit integration of uplift on carbon cycle evolution (Lefebvre et al., 2013).

6 Conclusion

10 In order to test the role that Neo-Tethys closure may have exerted on warm Paleocene/Early Eocene climate through CO_2 degassing at arc volcanoes, we have calculated the volume of buried pelagic sediments and associated volcanic CO_2 release during the LPEE and the EECO, and its impact on atmospheric $p\text{CO}_2$ and atmospheric temperature at that time. To do so, we have applied most recently published conver-
 15 gence rate parameters and decarbonation efficiencies to a simplified Neo-Tethyan geometry, and integrated calculated excess CO_2 fluxes in a state-of-the-art carbon cycle model (GEOCLIM).

We show that Neo-Tethys closure was able to bury significant volumes of pelagic sediments at that time. The inset of Indian continental subduction at 55–50 Ma may have potentially given rise to important volumes of excess CO_2 , through decarbonation
 20 of thick margin sediment accumulations. However, GEOCLIM modeling demonstrates that these volumes do not generally allow reaching $p\text{CO}_2$ (and thus temperatures) as high as those inferred from geochemical proxies. Atmospheric CO_2 concentration may have only been able to reach significantly high values during the EECO (up to
 25 770 ppm), but only if decarbonation efficiency was at its maximum at that time. This finding leads us to temper the impact of Neo-Tethys closure on the LPEE and the EECO, calling for additional sources of excess CO_2 .

Among these, GEOCLIM modeling suggests that in light of available published data, the volume of CO₂ released by Large Igneous Province volcanism was one order of magnitude too low to have had a significant impact on climate during the Paleocene and the Early Eocene. Other recently proposed mechanisms of CO₂ release such as a decrease of net organic carbon burial may have been more efficient in driving Paleocene/Eocene warming.

Appendix A

For each plate, subduction rates at each time step were corrected for convergence obliquity related to the orientation of the subduction trench using spherical trigonometric equations of the following form:

$$\text{Rate}_{\text{corr}} = \frac{\tan^{-1}(\tan A \cdot \cos B)}{t_2 - t_1} \quad (\text{A1})$$

$$\text{with } A = R_E \cdot \cos^{-1}(\sin \varphi_1 \cdot \sin \varphi_2 + \cos(\lambda_1 - \lambda_2) \cdot \cos \varphi_1 \cdot \cos \varphi_2) \quad (\text{A2})$$

$$B = \tan^{-1} \left(\frac{\sin(\lambda_2 - \lambda_1) \cdot \cos \varphi_2}{\cos \varphi_1 \cdot \sin \varphi_2 - \sin \varphi_1 \cdot \cos \varphi_2 \cdot \cos(\lambda_2 - \lambda_1) - (B_t - 90^\circ)} \right) \quad (\text{A3})$$

where Rate_{corr} is the corrected rate, (φ₁, λ₁) and (φ₂, λ₂) the Lat/Long decimal coordinates of two successive points, t₂ - t₁ the time step (0.5 Ma), R_E the Earth radius (6378.1 km) and B_t the trench bearing. Based on paleogeographic reconstructions of Barrier and Vrielynck (2008) and Agard et al. (2011), subduction trenches of Africa and Arabia below Eurasia were given constant bearings of 90 and 135° E, respectively. For India, orthogonal subduction rate was obtained assuming a bearing of 110° E, similar to the present orientation of the Indus-Yarlung Suture Zone between Indian and Asian rocks.

Did high Neo-Tethys subduction rates contribute to early Cenozoic warming?

G. Hoareau et al.

Title Page

Abstract

Introduction

Conclusions

References

Tables

Figures

◀

▶

◀

▶

Back

Close

Full Screen / Esc

Printer-friendly Version

Interactive Discussion



Appendix B:

For oceanic crust and pelagic sediments, the decarbonation efficiency (defined as number of moles of CO₂ emitted during a given time step of 0.5 Ma), $n\text{CO}_2(t)$, is expressed as:

$$n\text{CO}_2(t) = F_{\text{decarb}} \cdot \left(\frac{V_{\text{sed}}(t_0) \cdot \rho_{\text{sed}} \cdot (k_1 \cdot W_{\text{CaCO}_3\text{-sed}} + k_2 \cdot W_{\text{Corg}}) + k_1 \cdot V_{\text{crust}}(t_0) \cdot \rho_{\text{crust}} \cdot W_{\text{CaCO}_3\text{-crust}}}{M_{\text{CO}_2}} \right) \quad (\text{B1})$$

where $V_{\text{sed}}(t)$ and $V_{\text{crust}}(t)$ designate the volume of subducting sediments and crust (km³) for a given time step at $t_0 = t - \text{time-lag}$ (2 Ma), ρ_{sed} and ρ_{crust} their densities (g cm⁻³), $W_{\text{CaCO}_3\text{-sed}}$ and $W_{\text{CaCO}_3\text{-crust}}$ their weight fraction of carbonate, W_{Corg} the weight fraction of organic carbon in sediments, k_1 and k_2 are conversion unit factors ($k_1 = 4.161 \times 10^{14}$; $k_2 = 3.46 \times 10^{15}$), M_{CO_2} is the molecular weight of CO₂ (44 g mol⁻¹) and F_{decarb} is the decarbonation efficiency, defined as the mass percentage of carbon subducted as sedimentary carbonate, crustal carbonate and organic matter (carbon input), recycled as CO₂. Subducted volumes $V(t)$ were calculated as follows:

$$V(t_0) = H \cdot \left(\frac{L_{t[\text{Afr}]} \times \text{Rate}_{[\text{Afr}]}(t_0) + L_{t[\text{Arab}]} \times \text{Rate}_{[\text{Arab}]}(t_0) + L_{t[\text{Ind}]} \times \text{Rate}_{[\text{Ind}]}(t_0)}{t_s} \right) \quad (\text{B2})$$

where, respectively for subducted sediment or crust volumes $V(t)$, H is the sediment or crust thicknesses (km); $L_{t[\text{Afr}]}$, $L_{t[\text{Arab}]}$ and $L_{t[\text{Ind}]}$ are the subduction trench lengths of Africa, Arabia and India (km) and $\text{Rate}_{[\text{Afr}]}$, $\text{Rate}_{[\text{Arab}]}$ and $\text{Rate}_{[\text{Ind}]}$ the orthogonal subduction rates of Africa, Arabia and India beneath Eurasia at t_0 (km Ma⁻¹), and t_s is the time step (0.5 Ma in this study).

For continental crust and Indian margin sediments, the decarbonation efficiency (defined as number of moles of CO₂ emitted by subducting Indian continental margin

during a given time step of 0.5 Ma), $n\text{CO}_2(t)_{[\text{Ind}]}$, was calculated using an expression close to Eq. (B1):

$$n\text{CO}_2(t)_{[\text{Ind}]} = F_{\text{decarb}} \cdot \left(\frac{V_{\text{sed}}(t_0) \cdot \rho_{\text{sed}} \cdot (k_1 \cdot W_{\text{CaCO}_3\text{-sed}} + k_2 \cdot W_{\text{Corg}})}{M_{\text{CO}_2}} \right) \quad (\text{B3})$$

but where $V_{\text{sed}}(t)$, ρ_{sed} , $W_{\text{CaCO}_3\text{-sed}}$, W_{Corg} and F_{decarb} have numerical values specific of margin instead of pelagic sediments. In this case, $t = t_0$ and $V_{\text{sed}}(t)$ is represented as:

$$V_{\text{sed}}(t_0) = V_{\text{sed}}(t) = H_{\text{sed}} \cdot \left(\frac{L_{t[\text{Ind}]} \times \text{Rate}_{[\text{Ind}]}(t)}{t_s} \right) \quad (\text{B4})$$

Acknowledgements. F. Behar and T. Parra are thanked for helpful discussions. G. Hoareau and B. Bomou benefited from Post-doctoral grants from INSU- and INEE-CNRS.

References

- Agard, P., Omrani, J., Jolivet, L., Whitechurch, H., Vrielynck, B., Spakman, W., Monié, P., Meyer, B., and Wortel, R.: Zagros orogeny: a subduction-dominated process, *Geol. Mag.*, 148, 692–725, 2011.
- Alt, J. C. and Teagle, D. A. H.: The uptake of carbon during alteration of ocean crust: *Geochim. Cosmochim. Acta*, 63, 1527–1535, 1999.
- Alvarez, W.: Protracted continental collisions argue for continental plates driven by basal traction, *Earth Planet. Sc. Lett.*, 296, 434–442, doi:10.1016/j.epsl.2010.05.030, 2010.
- Barrier, E. and Vrielynck, B.: *Paleotectonic Maps of the Middle East: Middle East Basins Evolution Programme, CCGM-CGMW, Paris, 2008.*
- Beck, R. A., Burbank, D. W., Sercombe, W. J., Olson, T. L., and Khan, A. M.: Organic carbon exhumation and global warming during the early Himalayan collision, *Geology*, 23, 387–390, doi:10.1130/0091-7613(1995)023<0387:OCEAGW>2.3.CO;2, 1995.
- Becker, J. A., Bickle, M. J., Galy, A., and Holland, T. J. B., Himalayan metamorphic CO_2 fluxes: quantitative constraints from hydrothermal springs, *Earth Planet. Sc. Lett.*, 265, 616–629, 2008.

Did high Neo-Tethys subduction rates contribute to early Cenozoic warming?

G. Hoareau et al.

[Title Page](#)[Abstract](#)[Introduction](#)[Conclusions](#)[References](#)[Tables](#)[Figures](#)[Back](#)[Close](#)[Full Screen / Esc](#)[Printer-friendly Version](#)[Interactive Discussion](#)

Dupont-Nivet, G., Lippert, P., van Hinsbergen, D. J. J., Meijers, M. J. M., and Kapp, P.: Paleolatitude and age of the Indo-Asia collision: paleomagnetic constraints, *Geophys. J. Int.*, 182, 1189–1198, 2010.

Edmond, J. M. and Huh, Y.: Non-steady state carbonate recycling and implications for the evolution of atmospheric $p\text{CO}_2$, *Earth Planet. Sc. Lett.*, 216, 125–139, doi:10.1016/S0012-821X(03)00510-7, 2003.

Eldholm, O. and Thomas, E.: Environmental impact of volcanic margin formation, *Earth Planet. Sc. Lett.*, 117, 319–329, doi:10.1016/0012-821X(93)90087-P, 1993.

Engebretson, D. C., Kelley, K. P., Cashman, H. J., and Richards, M. A.: 180 million years of subduction, *GSA Today*, 2, 93–95, 1992.

England, P. C. and Katz, R. F.: Melting above the anhydrous solidus controls the location of volcanic arcs, *Nature*, 467, 700–703, doi:10.1038/nature09417, 2010.

Evans, M. J., Derry, L. A., and France-Lanord, C.: Degassing of metamorphic carbon dioxide from the Nepal Himalaya, *Geochem. Geophys. Geosy.*, 9, Q04021, doi:10.1029/2007GC001796, 2008.

Eyuboglu, Y., Santosh, M., Dudas, F. O., Chung, S. L., and Akaryali, E.: Migrating magmatism in a continental arc: geodynamics of the Eastern Mediterranean revisited, *J. Geodyn.*, 52, 2–15, 2011.

Friedrich, O., Norris, R. D., and Erbacher, J.: Evolution of middle to Late Cretaceous oceans – a 55 m.y. record of Earth's temperature and carbon cycle, *Geology*, 40, 107–110, doi:10.1130/G32701.1, 2012.

Froelich, F. and Misra, S.: Was the Late Paleocene–Early Eocene hot because Earth was flat? An ocean lithium isotope view of mountain building, continental weathering, carbon dioxide, and Earth's Cenozoic climate, *Oceanography*, 27, 36–49, doi:10.5670/oceanog.2014.06, 2014

Gaina, C., van Hinsbergen, D. J. J., and Spakman, W.: Tectonic interactions between India and Arabia since the Jurassic reconstructed from marine geophysics, ophiolite geology, and seismic tomography, *Tectonics*, 34, 875–906, doi:10.1002/2014TC003780, 2015.

Garzanti, E. and Hu, X.: Latest Cretaceous Himalayan tectonics: obduction, collision or Deccan-related uplift?, *Gondwana Res.*, 28, 165–178, 2014.

Gnos, E., Immenhauser, A., and Peters, T.: Late Cretaceous/Early Tertiary convergence between the Indian and Arabian plates recorded in ophiolites and related sediments, *Tectonophysics*, 271, 1–20, 1997.

Did high Neo-Tethys subduction rates contribute to early Cenozoic warming?

G. Hoareau et al.

Title Page

Abstract

Introduction

Conclusions

References

Tables

Figures



Back

Close

Full Screen / Esc

Printer-friendly Version

Interactive Discussion



Goddéris, Y. and Joachimski, M. M.: Global change in the Late Devonian: modelling the Frasnian–Famennian short-term carbon isotope excursions, *Palaeogeogr. Palaeoecol.*, 202, 309–329, 2004.

Goddéris, Y., Donnadiou, Y., Tombozafy, M., and Dessert, C.: Shield effect on continental weathering: implication for climatic evolution of the Earth at the geological time-scale, *Geoderma*, 145, 439–448, 2008.

Goddéris, Y., Donnadiou, Y., Le Hir, G., Lefebvre, V., and Nardin, E.: The role of palaeogeography in the Phanerozoic history of atmospheric CO₂ and climate, *Earth-Sci. Rev.*, 128, 122–138, 2014.

Gorman, P. J., Kerrick, D. M., and Connolly, J. A. D.: Modeling open system metamorphic decarbonation of subducting slabs, *Geochem. Geophys. Geosy.*, 7, Q04007, doi:10.1029/2005GC001125, 2006.

Guillot, S., Maheo, G., de Sigoyer, J., Hattori, K. H., and Pecher, A.: Tethyan and Indian subduction viewed from the Himalayan high- to ultrahigh-pressure metamorphic rocks, *Tectonophysics*, 451, 225–241, 2008.

Hall, R.: Late Jurassic-Cenozoic reconstructions of the Indonesian region and the Indian Ocean, *Tectonophysics*, 570–571, 1–41, doi:10.1016/j.tecto.2012.04.021, 2012.

Hancock, H. J. L., Dickens, G. R., Thomas, E., and Blake, K. L.: Reappraisal of early Paleogene CCD curves: foraminiferal assemblages and stable carbon isotopes across the carbonate facies of Perth Abyssal Plain, *Int. J. Earth Sci.*, 96, 925–946, doi:10.1007/s00531-006-0144-0, 2007.

Hébert, R., Bezard, R., Guilmette, C., Dostal, J., Wang, C. S., and Liu, Z. F.: The Yarlung Zangbo Ophiolites from Nanga Parbat to Namche Barwa syntaxes, Southern Tibet: a synthesis of petrology, geochemistry and ages with incidences on geodynamic reconstructions of the Neo-Tethys, in: *Plate Tectonics of Asia: Geological and Geophysical Constraints*, edited by: Zhao, X. X., Xiao, W. J., Wang, C. S., and Hébert, R., *Gondwana Res.*, 22, 377–397, 2012.

Hilting, A. K., Kump, L. R., and Bralower, T. J.: Variations in the oceanic vertical carbon isotope gradient and their implications for the Paleocene-Eocene biological pump, *Paleoceanography*, 23, PA3222, doi:10.1029/2007PA001458, 2008.

Hilton, D. R., Fischer, T. P., and Marty, B.: Noble gases and volatile recycling at subduction zones, in: *Noble Gases in Cosmochemistry and Geochemistry*, edited by: Porcelli, D., Bal-

Did high Neo-Tethys subduction rates contribute to early Cenozoic warming?

G. Hoareau et al.

Title Page

Abstract

Introduction

Conclusions

References

Tables

Figures



Back

Close

Full Screen / Esc

Printer-friendly Version

Interactive Discussion



Komar, N., Zeebe, R. E., and Dickens, G. R.: Understanding long-term carbon cycle trends: the late Paleocene through the early Eocene, *Paleoceanography*, 28, 650–662, doi:10.1002/palo.20060, 2013.

Kroeger, K. F. and Funnel, R. H.: Warm Eocene climate enhanced petroleum generation from Cretaceous source rocks: a potential climate feedback mechanism?, *Geophys. Res. Lett.*, 39, L04701, doi:10.1029/2011GL050345, 2012.

Kroenke, L., Berger, W., Janecek, T. et al.: Proceedings of the Ocean Drilling Program, Initial Reports, vol. 130, Ocean Drilling Program, College Station, Texas, doi:10.2973/odp.proc.ir.130.1991, 1991.

Kurtz, A., Kump, L. R., Arthur, M. A., Zachos, J. C., and Paytan, A.: Early Cenozoic decoupling of the global carbon and sulfur cycles, *Paleoceanography*, 18, 1090, doi:10.1029/2003PA000908, 2003.

Lee, C.-T. A., Shen, B., Slotnick, B. S., Liao, K., Dickens, G. R., Yokoyama, Y., Lenardic, A., Dasgupta, R., Jellinek, M., Lackey, J. S., Schneider, T., and Tice, M. M.: Continental arc–island arc fluctuations, growth of crustal carbonates, and long-term climate change, *Geosphere*, 9, 21–36, doi:10.1130/GES00822.1, 2013.

Leech, M. L., Singh, S., Jain, A. K., Klemperer, S. L., and Manickavasagam, R. M.: The onset of India–Asia continental collision: early, steep subduction required by the timing of UHP metamorphism in the western Himalaya, *Earth Planet. Sc. Lett.*, 234, 83–97, 2005.

Lefebvre, V., Donnadieu, Y., Godd eris, Y., Fluteau, F., and Hubert-The iou, L.: Was the Antarctic glaciation delayed by a high degassing rate during the early Cenozoic?, *Earth Planet. Sc. Lett.*, 371–372, 203–211, 2013.

Leon-Rodr guez, L. and Dickens, G. R.: Constraints on ocean acidification associated with rapid and massive carbon injections: the early Paleogene record at ocean drilling program site 1215, equatorial Pacific Ocean, *Palaeogeogr. Palaeoclimatol.*, 298, 409–420, 2010.

Liu, G. and Einsele, G.: Sedimentary history of the Tethyan basin in the Tibetan Himalayas, *Geol. Rundsch.*, 83, 32–61, 1994.

Marquer, D., Mercolli, I., and Peters, T.: Early Cretaceous intra-oceanic rifting in the proto-Indian Ocean recorded in the Masirah Ophiolite, Sultanate of Oman, *Tectonophysics*, 292, 1–16, 1998.

Massonne, H.-J.: Phase relations and dehydration behaviour of calcareous sediments at very-low to low grade metamorphic conditions, *Period. Mineral.*, 79, 21–43, 2010.

Did high Neo-Tethys subduction rates contribute to early Cenozoic warming?

G. Hoareau et al.

Title Page

Abstract

Introduction

Conclusions

References

Tables

Figures

◀

▶

◀

▶

Back

Close

Full Screen / Esc

Printer-friendly Version

Interactive Discussion



- McCourt, W., M. Crow, E. Cobbing, and Amin, T.: Mesozoic and Cenozoic plutonic evolution of SE Asia: evidence from Sumatra, Indonesia, *Special Publications, Geol. Soc. London*, 106, 321–335, 1996.
- McQuarrie, N. and van Hinsbergen, D. J. J.: Retro-deforming the Arabia–Eurasia collision zone: age of collision versus magnitude of continental subduction, *Geology*, 41, 315–318, doi:10.1130/G33591.1, 2013.
- Menzies, M. A., Klemperer, S. L., Ebinger, C. J., and Baker, J.: Characteristics of volcanic rifted margins, in: *Volcanic Rifted Margins*, 362, edited by: Menzies, M. A., Klemperer, S. L., Ebinger, C. J., and Baker, J., *Geological Society of America Special Paper*, 1–14, doi:10.1130/0-8137-2362-0.1, 2002.
- Misra, S. and Froelich, P. N.: Lithium isotope history of Cenozoic seawater: changes in silicate weathering and reverse weathering, *Science*, 335, 818–823, doi:10.1126/science.1214697, 2012.
- Mouthereau, F.: Timing of uplift in the Zagros belt/Iranian plateau and accommodation of late Cenozoic Arabia–Eurasia convergence, *Geol. Mag.*, 148, 726–738, doi:10.1017/s0016756811000306, 2011.
- Müller, R. D., Sdrolias, M., Gaina, C., and Roest, W. R.: Age, spreading rates, and spreading asymmetry of the world’s ocean crust, *Geochem. Geophys. Geosy.*, 9, Q04006, doi:10.1029/2007GC001743, 2008.
- Muttoni, G., Mattei, M., Balini, M., Zanchi, A., Gaetani, M., and Berra, F.: The drift history of Iran from the Ordovician to the Triassic, in: *South Caspian to Central Iran Basins*, edited by: Brunet, M.-F., Wilmsen, M., and Granath, J. W., *Special Publications, Geological Society of London*, 7–29, 2009.
- Najman, Y., Oliver, G., Parrish, R., Vezzoli, G., Appel, E., Boudagher-Fadel, M., Bown, P., Carter, A., Garzanti, E., Godin, L., Han, J., and Liebke, U.: Timing of India–Asia collision: geological, biostratigraphic, and palaeomagnetic constraints, *J. Geophys. Res.-Sol. Ea.*, 115, B12416, doi:10.1029/2010JB007673, 2010.
- Nesbitt, B., Mendoza, C., and Kerrick, D.: Surface fluid convection during cordilleran extension and the generation of metamorphic CO₂ contributions to Cenozoic atmospheres, *Geology*, 23, 99–101, 1995.
- Okay, A. I. and Şahintürk, Ö.: Geology of the Eastern Pontides, in: *Regional and Petroleum Geology of the Black Sea and Surrounding Region*, edited by: Robinson, A. G., *AAPG Memoir*, 68, 291–311, 1997.

Did high Neo-Tethys subduction rates contribute to early Cenozoic warming?

G. Hoareau et al.

Title Page

Abstract

Introduction

Conclusions

References

Tables

Figures



Back

Close

Full Screen / Esc

Printer-friendly Version

Interactive Discussion

Orme, D. A., Carrapa, B., and Kapp, P. K.: Sedimentology, provenance and geochronology of the western Xigaze Forearc, Southern Tibet, *Basin Res.*, 27, 387–411, doi:10.1111/bre.12080, 2014.

Pälike, H., Lyle, M.W., Nishi, H., Raffi, I., Ridgwell, A., Gamage, K., Klaus, A., Acton, G., Anderson, L., Backman, J., Baldauf, J., Beltran, C., Bohaty, S. M., Bown, P., Busch, W., Channell, J. E. T., Chun, C. O. J., Delaney, M., Dewangan, P., Dunkley Jones, T., Edgar, K. M., Evans, H., Fitch, P., Foster, G. L., Gussone, N., Hasegawa, H., Hathorne, E. C., Hayashi, H., Herrle, J. O., Holbourn, A., Hovan, S., Hyeong, K., Iijima, K., Ito, T., Kamikuri, S., Kimoto, K., Kuroda, J., Leon-Rodriguez, L., Malinverno, A., Moore, T. C., Murphy, B. H., Murphy, D.P., Nakamura, H., Ogane, K., Ohneiser, C., Richter, C., Robinson, R., Rohling, E. J., Romero, O., Sawada, K., Scher, H., Schneider, L., Sluijs, A., Takata, H., Tian, J., Tsujimoto, A., Wade, B. S., Westerhold, T., Wilkens, R., Williams, T., Wilson, P. A., Yamamoto, Y., Yamamoto, S., Yamazaki, T., and Zeebe, R. E.: A Cenozoic record of the equatorial Pacific carbonate compensation depth, *Nature*, 488, 609–614, 2012.

Park, J. and Royer, D. L.: Geologic constraints on the glacial amplification of Phanerozoic climate sensitivity, *Am. J. Sci.*, 311, 1–26, doi:10.2475/01.2011.01, 2011.

Peacock, S. M.: Thermal structure and metamorphic evolution of subducting slabs, in: *Inside the Subduction Factory*, edited by: Eiler, J. M., Geophysical Monograph Ser. American Geophysical Union, Washington, D.C., 7–22, 2003.

Reagan, M. K., McClelland, W. C., Girard, G., Goff, K. R., Peate, D. W., Ohara, Y., and Stern, R. J.: The geology of the southern Mariana fore-arc crust: implications for the scale of Eocene volcanism in the western Pacific, *Earth Planet. Sc. Lett.*, 380, 41–51, doi:10.1016/j.epsl.2013.08.013, 2013.

Ricou, L. M.: Tethys reconstructed: plates, continental fragments and their boundaries since 260 Ma from Central America to South-eastern Asia, *Geodin. Acta*, 7, 169–218, 1994.

Rohrmann, A., Kapp, P., Carrapa, B., Reiners, P. W., Guynn, J., Ding, L., and Heizler, M.: Thermochronologic evidence for plateau formation in central Tibet by 45 Ma, *Geology*, 40, 187–190, doi:10.1130/G32530.1, 2012.

Rosenbaum, G., Lister, G. S., and Duboz, C.: Relative motions of Africa, Iberia and Europe during Alpine orogeny, *Tectonophysics*, 359, 117–129, doi:10.1016/S0040-1951(02)00442-0, 2002.

Did high Neo-Tethys subduction rates contribute to early Cenozoic warming?

G. Hoareau et al.

[Title Page](#)

[Abstract](#)

[Introduction](#)

[Conclusions](#)

[References](#)

[Tables](#)

[Figures](#)



[Back](#)

[Close](#)

[Full Screen / Esc](#)

[Printer-friendly Version](#)

[Interactive Discussion](#)



Sanchez, V. I., Murphy, M. A., Robinson, A. C., Lapen, T. L., and Heizler, M. T.: Tectonic evolution of the India–Asia suture zone since Middle Eocene time, Lopukangri area, south-central Tibet, *J. Asian Earth Sci.*, 62, 205–220, 2013.

Sciunnach, D. and Garzanti, E.: Subsidence history of the Tethys Himalaya, *Earth-Sci. Rev.*, 25, 179–198, 2012.

Searle, M. and Cox, J.: Tectonic setting, origin, and obduction of the Oman ophiolite, *Geol. Soc. Am. Bull.*, 111, 104–122, 1999.

Sengör A. M. C., Altiner, D., Cin, A., Ustaömer T., and Hsü, K. J.: Origin and assembly of the Tethyside orogenic collapse at the expense of Gondwana Land, in: *Gondwana and Tethys*, edited by: Audley-Charles, M. G. and Hallam, A., Special Publications, Geological Society of London, 37, 119–181, 1988.

Shackleton, N. J. and Kennett, J. P.: Paleo-temperature history of the Cenozoic and the initiation of Antarctic glaciation: oxygen and carbon isotope analyses in DSDP Sites 277, 279 and 281, *Initial Rep. Deep Sea*, 29, 743–755, 1975.

Skelton, A.: Flux rates for water and carbon during greenschist facies metamorphism, *Geology*, 39, 43–46, doi:10.1130/G31328.1, 2011.

Slotnick, B. S., Laurentano, V., Backman, J., Dickens, G. R., Sluijs, A., and Lourens, L.: Early Paleogene variations in the calcite compensation depth: new constraints using old borehole sediments from across Ninetyeast Ridge, central Indian Ocean, *Clim. Past*, 11, 473–493, doi:10.5194/cp-11-473-2015, 2015.

Stampfli, G. M. and Borel, G. D.: A plate tectonic model for the Paleozoic and Mesozoic constrained by dynamic plate boundaries and restored synthetic oceanic isochrons, *Earth Planet. Sc. Lett.*, 196, 17–33, doi:10.1016/S0012-821X(01)00588-X, 2002.

Sykes, T. J. S.: A correction for sediment load upon the ocean floor: uniform versus varying sediment density estimations – implications for isostatic correction, *Mar. Geol.*, 133, 35–49, doi:10.1016/0025-3227(96)00016-3, 1996.

Turner, S. P.: On the time-scales of magmatism at island-arc volcanoes, *Philos. T. Roy. Soc. A*, 360, 2853–2871, doi:10.1098/rsta.2002.1060, 2002.

van Hinsbergen, D. J. J., Hafkenscheid, E., Spakman, W., Meulenkamp, J. E., and Wortel, M. J. R.: Nappe stacking resulting from subduction of oceanic and continental lithosphere below Greece, *Geology*, 33, 325–328, 2005.

van Hinsbergen, D. J. J., Steinberger, B., Doubrovine, P. V., and Gassmöller, R.: Acceleration and deceleration of India–Asia convergence since the Cretaceous: roles of mantle plumes

Did high Neo-Tethys subduction rates contribute to early Cenozoic warming?

G. Hoareau et al.

[Title Page](#)

[Abstract](#)

[Introduction](#)

[Conclusions](#)

[References](#)

[Tables](#)

[Figures](#)



[Back](#)

[Close](#)

[Full Screen / Esc](#)

[Printer-friendly Version](#)

[Interactive Discussion](#)



and continental collision, *J. Geophys. Res.*, 116, B06101, doi:10.1029/2010JB008051, 2011a.

van Hinsbergen, D. J. J., Kapp, P., Dupont-Nivet, G., Lippert, P. C., DeCelles, P., and Torsvik, T.: Restoration of Cenozoic deformation in Asia and the size of Greater India, *Tectonics*, 30, TC5003, doi:10.1029/2010JB008051, 2011b.

van Hinsbergen, D. J. J., Lippert, P. C., Dupont-Nivet, G., McQuarrie, N., Doubrovine, P. V., Spakman, W., and Torsvik, T. H.: Greater India Basin hypothesis and a two-stage Cenozoic collision between India and Asia, *P. Natl. Acad. Sci. USA*, 109, 7659–7664, doi:10.1073/pnas.1117262109, 2012.

Van Der Meer, D. G., Zeebe, R. E., van Hinsbergen, D. J. J., Sluijs, A., Spakman, W., and Torsvik, T. H.: Plate tectonic controls on atmospheric CO₂ levels since the Triassic, *P. Natl. Acad. Sci. USA*, 111, 4380–4385, doi:10.1073/pnas.1315657111, 2014.

Vigier, N. and Godd ris, Y.: A new approach for modeling Cenozoic oceanic lithium isotope paleo-variations: the key role of climate, *Clim. Past*, 11, 635–645, doi:10.5194/cp-11-635-2015, 2015

Walker, J. C. G., Hays, P. B., and Kasting, J. F.: A negative feedback mechanism for the long-term stabilization of Earth's surface temperature, *J. Geophys. Res.*, 86, 9776–9782, 1981.

Watts, A. B. and Thorne, J. A.: Tectonics, global changes in sea-level and their relationship to stratigraphic sequences at the U.S. Atlantic continental margin, *Mar. Petrol. Geol.*, 1, 319–339, 1984.

Whittaker, J. M., M ller, R. D., Sdrolias, M., and Heine, C.: Sunda-Java trench kinematics, slab window formation and overriding plate deformation since the Cretaceous, *Earth Planet. Sc. Lett.*, 255, 445–457, doi:10.1016/j.epsl.2006.12.031, 2007.

Zachos, J. C., Pagani, M., Sloan, L., Thomas, E., and Billups, K.: Rhythms, and aberrations in global climate 65 Ma to present, *Science*, 292, 686–693, doi:10.1126/science.1059412, 2001.

Zachos, J. C., Dickens, G. R., and Zeebe, R. E.: An early Cenozoic perspective on greenhouse warming and carbon-cycle dynamics: year of planet Earth, *Nature*, 451, 279–283, doi:10.1038/nature06588, 2008.

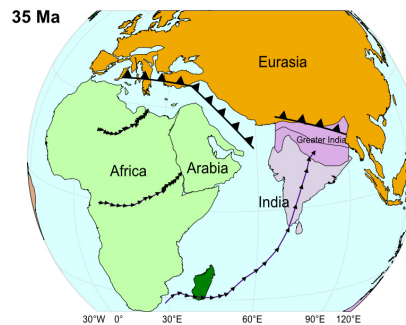
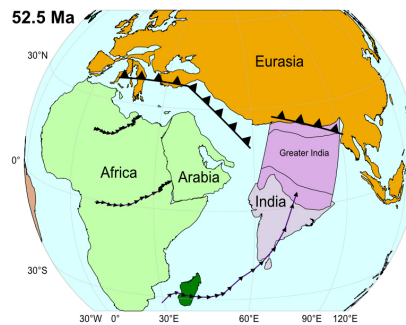
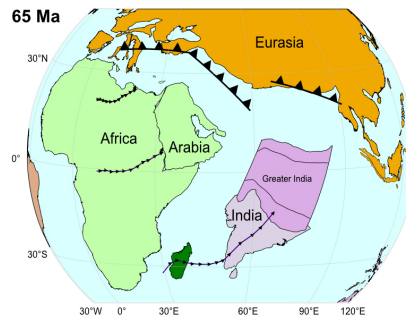
Zheng, Y.-F.: Metamorphic chemical geodynamics in continental subduction zones, *Chem. Geol.*, 328, 5–48, 2012.

CPD

11, 2847–2888, 2015

Did high Neo-Tethys subduction rates contribute to early Cenozoic warming?

G. Hoareau et al.


[Title Page](#)
[Abstract](#)
[Introduction](#)
[Conclusions](#)
[References](#)
[Tables](#)
[Figures](#)

[Back](#)
[Close](#)
[Full Screen / Esc](#)
[Printer-friendly Version](#)
[Interactive Discussion](#)


Figure 1. Simplified paleogeographic maps showing the positions of Africa, Arabia, India and Eurasia at 65, 52.5 and 35 Ma (3-D Globe projection; rotation poles of Müller et al., 2008, fixed Eurasian frame). The bearing/length of subduction trenches used in the model are represented as black lines, while possible intra-oceanic subduction zones leading to obduction events (not considered in the model) are reported as dashed lines. Flow lines (65–35 Ma) of three points representative of the central syntaxis of each plate are also reported (see text for present locations). Extension of Greater India during the Upper Cretaceous is based on the Greater India Basin hypothesis of Van Hinsbergen et al. (2012).

Did high Neo-Tethys subduction rates contribute to early Cenozoic warming?

G. Hoareau et al.

[Title Page](#)[Abstract](#)[Introduction](#)[Conclusions](#)[References](#)[Tables](#)[Figures](#)[Back](#)[Close](#)[Full Screen / Esc](#)[Printer-friendly Version](#)[Interactive Discussion](#)

Did high Neo-Tethys subduction rates contribute to early Cenozoic warming?

G. Hoareau et al.

[Title Page](#)

[Abstract](#)

[Introduction](#)

[Conclusions](#)

[References](#)

[Tables](#)

[Figures](#)



[Back](#)

[Close](#)

[Full Screen / Esc](#)

[Printer-friendly Version](#)

[Interactive Discussion](#)

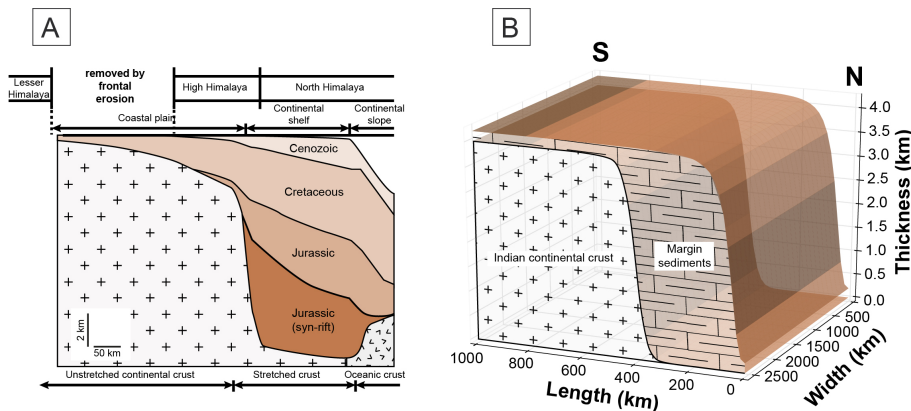


Figure 2. (a) Geometry of the Eastern US Atlantic coastal margin showing analogous positions for tectonic units of Indian passive margin (modified from Brookfield, 1993). (b) Geometry of Indian margin used in Carbonate Subduction Factory Model (CSFM).

Did high Neo-Tethys subduction rates contribute to early Cenozoic warming?

G. Hoareau et al.

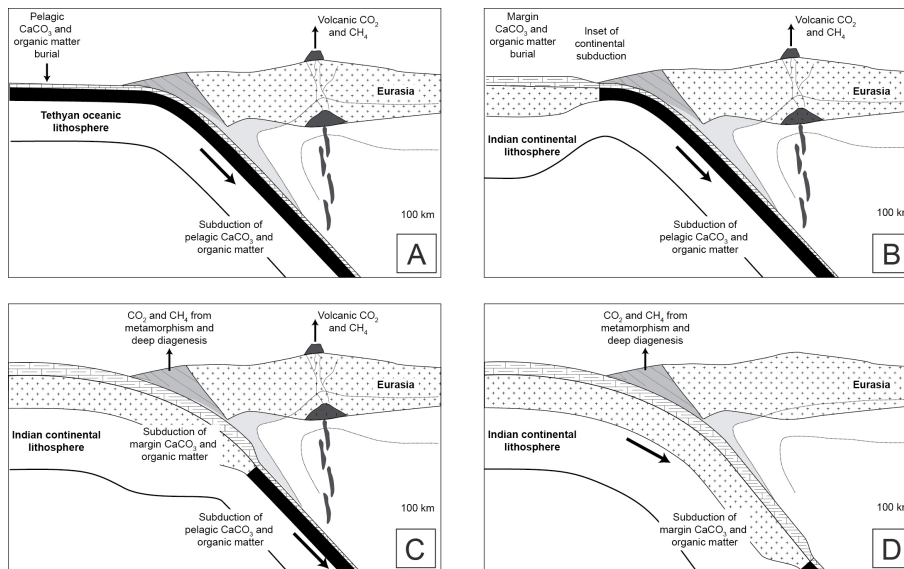
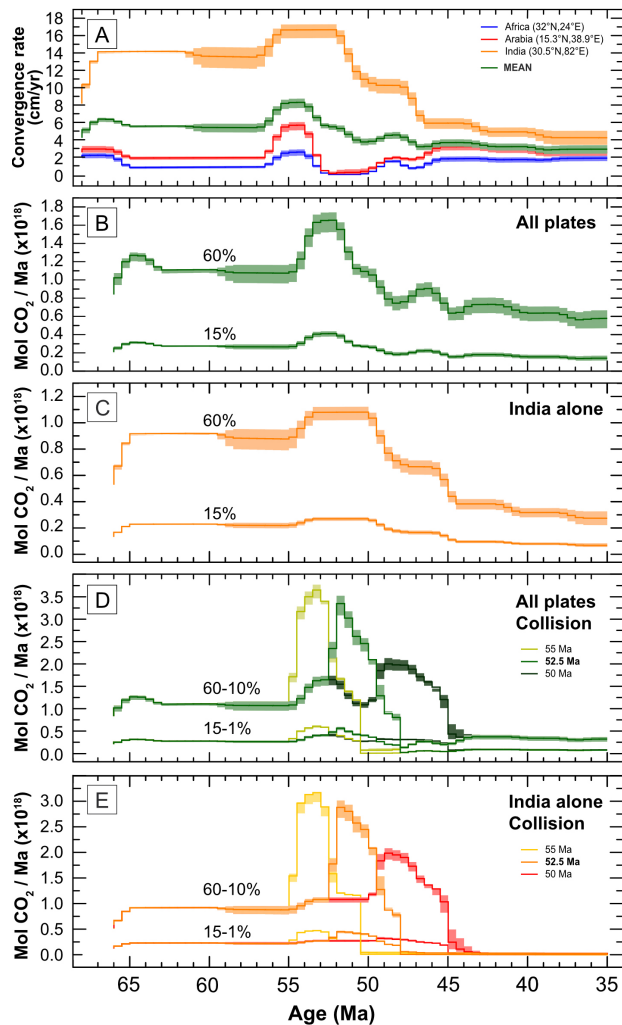


Figure 3. Sketches illustrating the carbon input and outputs considered in the model during subduction. **(a)** General sketch for subduction of oceanic crust and pelagic sediments (Africa, Arabia and India before Indian continental subduction). Carbon deposited as carbonate and organic carbon in pelagic sediments, as well as crustal carbonate, is partly recycled at sub-arc depth and incorporated in arc magmas. **(b)** Similar sketch at the inset of Indian continental subduction. **(c)** Subduction of northern Indian margin before it reaches sub-arc depth. Carbon originating from low-grade metamorphism of Indian margin sediments is partly released to the atmosphere, making additional greenhouse gas to that released at arc volcanoes. **(d)** Arc volcanism stops as Indian continental crust reaches sub-arc depth.

[Title Page](#)
[Abstract](#)
[Introduction](#)
[Conclusions](#)
[References](#)
[Tables](#)
[Figures](#)
[Back](#)
[Close](#)
[Full Screen / Esc](#)
[Printer-friendly Version](#)
[Interactive Discussion](#)

Did high Neo-Tethys subduction rates contribute to early Cenozoic warming?

G. Hoareau et al.



Title Page

Abstract

Introduction

Conclusions

References

Tables

Figures



Back

Close

Full Screen / Esc

Printer-friendly Version

Interactive Discussion



Figure 4. (a) Calculated mean Tethyan subduction rate over the period 65–35 Ma, compared with individual subduction rates of Africa, Arabia and India beneath Eurasia. Upper and lower limits of the shaded areas are maximum and minimum velocities, respectively, corresponding to points located on the western and eastern syntaxes of each plate. Rates calculated using rotation parameters of van Hinsbergen et al. (2011a, b). **(b)** Amount of CO₂ produced by the subduction of the Tethys under Eurasia for the same period (green lines), using plate velocities calculated from van Hinsbergen et al. (2011a), for 15 and 60 % efficiencies. Upper and lower limits of the shaded areas are maximum and minimum gas flux rates computed for each efficiency, respectively; **(c)** same as **(b)** but for Indian only. **(d)** Same as **(b)** but including Indian margin subduction at 55, 52.5 and 50 Ma. **(e)** Same as **(d)** but for India only.

Did high Neo-Tethys subduction rates contribute to early Cenozoic warming?

G. Hoareau et al.

Title Page

Abstract

Introduction

Conclusions

References

Tables

Figures



Back

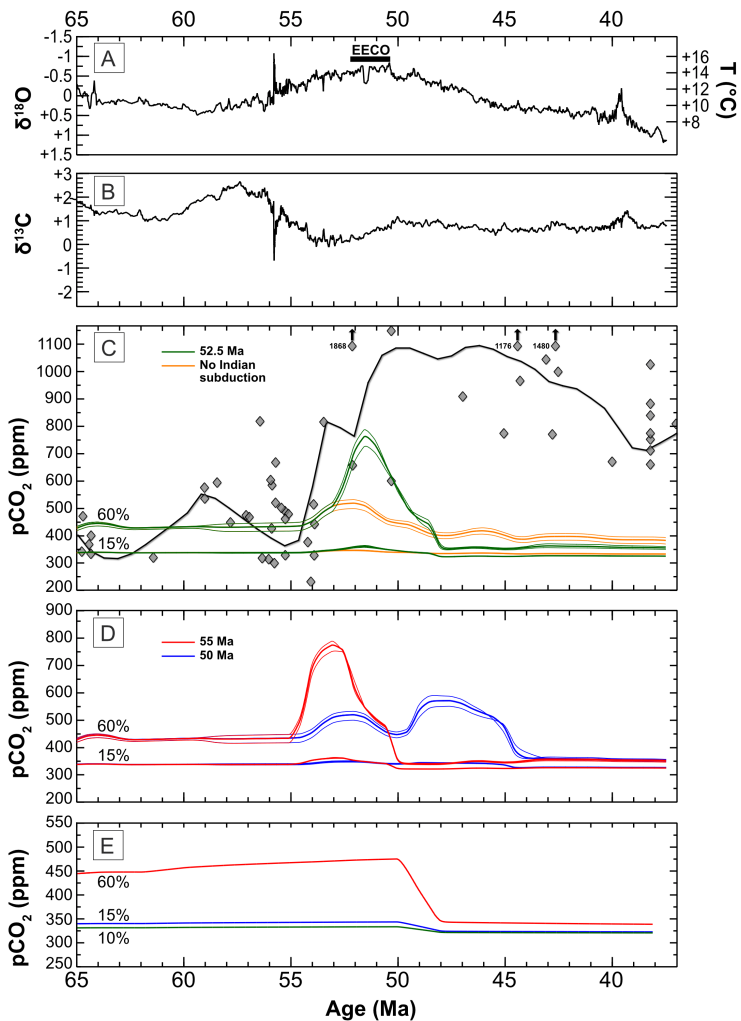
Close

Full Screen / Esc

Printer-friendly Version

Interactive Discussion





Did high Neo-Tethys subduction rates contribute to early Cenozoic warming?

G. Hoareau et al.

[Title Page](#)

[Abstract](#) | [Introduction](#)

[Conclusions](#) | [References](#)

[Tables](#) | [Figures](#)

[◀](#) | [▶](#)

[◀](#) | [▶](#)

[Back](#) | [Close](#)

[Full Screen / Esc](#)

[Printer-friendly Version](#)

[Interactive Discussion](#)



Figure 5. (a, b) Global oceanic benthic $\delta^{18}\text{O}$ **(a)** and $\delta^{13}\text{C}$ **(b)** foraminiferal compilation based on data from Cramer et al. (2009). Data were smoothed using 10-point running average. Temperatures calculated from $\delta^{18}\text{O}$ values assume an ice-free world (after Komar et al., 2013). **(c)** GEOCLIM modeling results of atmospheric $p\text{CO}_2$ resulting from excess CO_2 release associated with Neo-Tethys closure using plate velocities calculated from van Hinsbergen et al. (2011a), for 15 and 60% decarbonation efficiencies. Orange curves assume no Indian continental subduction, green lines correspond to an initiation of Indian continental subduction at 52.5 Ma. Individual (grey diamonds) and mean (black line) atmospheric $p\text{CO}_2$ recorded by paleoproxies are also shown (from Beerling and Royer, 2011). Black arrows and associated number refer to $p\text{CO}_2$ values too high to be displayed. **(d)** Same as **(c)** but for an initiation of Indian continental subduction at 55 Ma (red curves) and 50 Ma (blue curves). **(e)** GEOCLIM modeling results of atmospheric $p\text{CO}_2$ resulting from excess CO_2 release as calculated from data of Kent and Muttoni (2013) using efficiencies of 10, 15 and 60%.

CPD

11, 2847–2888, 2015

Did high Neo-Tethys subduction rates contribute to early Cenozoic warming?

G. Hoareau et al.

Title Page

Abstract

Introduction

Conclusions

References

Tables

Figures

◀

▶

◀

▶

Back

Close

Full Screen / Esc

Printer-friendly Version

Interactive Discussion

